

In vivo dynamic contrast enhanced MRI of novel contrast agents targeted to the estrogen receptor

A. Pais¹, G. Chidambaram², I. Biton³, R. Margalit¹, D. Milstein², and H. Degani¹

¹Biological Regulation, Weizmann Institute of Science, Rehovot, Israel, ²Organic Chemistry, Weizmann Institute of Science, Rehovot, Israel, ³Veterinary Resources, Weizmann Institute of Science, Rehovot, Israel

Purpose: to investigate the specific binding of novel estrogen receptor targeted contrast agents to the estrogen receptor *in vivo* and examine the ability of these agents to serve as molecular probes for detecting estrogen receptor in breast cancers.

Introduction: It has been established that estrogen regulation has a pivotal role in the etiology and progression of breast cancer. The level of the estrogen receptor is an important biomarker for assessment of the prognosis of breast cancer patients and serves to predict response to adjuvant endocrine therapy. The currently most common method to determine ER presence in breast cancer tumors in the clinical setting is immunostaining of ER with specific antibodies. This *ex vivo* method suffers from various limitations and lacks standardization among different laboratories which can be overcome by a non-invasive molecular imaging technique that utilizes probes that bind specifically to ER and augment signal enhancement upon binding. Previously we have reported investigations of the solution chemistry, binding to ER, interaction in cells and biological activity of two novel ER targeted contrast agents gadolinium-pyridiniumtetraacetic acid conjugated to 17 β -estradiol (EPTA-Gd) or tamoxifen (TPTA-Gd) (1-3), (Figure 1). Here we describe *in vivo* dynamic contrast enhanced studies of these two probes in ER-positive versus ER-negative human breast cancer tumors.

Methods: EPTA-Gd, and TPTA-Gd as well as the contrast agent moiety PTA-Gd were newly synthesized using methods described earlier (1,2). Tumors were derived from ER-negative human MDA-MB-231 breast cancer cells and from the same cells after turning them into ER-positive cells by stable transfection with Tetracycline inducible ER. The cells were inoculated into the left and right mammary fat pad, respectively, of female CB-17 SCID mice, 6-7 weeks old that were ovariectomized. ER expression was induced by supplementing the drinking water with 0.2 mg/ml doxycyclin in 3% sucrose. 2-4 weeks after cell implantation, the mice were sequentially scanned by MRI. Images were acquired on a 9.4T Biospec AVANCE II spectrometer (Bruker). Mice were anesthetized during MRI scans by inhalation of 1-2% isoflurane in a gas mixture of N₂:O₂ (7:3). T1 relaxation rates in blood and tumors were measured by a spin echo sequence varying TRs. Anatomical images revealing histopathological features were obtained using a multi-slice RARE T2-weighted sequence with TE/TR 42/3000 ms. Dynamic experiments consisted of recording four pre-contrast and consecutive post-contrast at temporal resolution of 3.5 min, T1-weighted, 3D gradient-echo images with TE/TR 2.5/15 ms; flip angle $\alpha=40^\circ$; matrix 256x256x16; FOV 4x4x1.92 cm³; spatial resolution 0.156x0.156x1.2 mm³. Contrast agents were injected as a bolus into the tail vein of the mice, at doses of: GdDTPA - 0.4 mmol/kg, PTA-Gd - 0.15 mmol/kg, TPTA-Gd - 0.075 mmol/kg and EPTA-Gd - 0.03-0.1 mmol/kg. Changes in the blood concentration were examined either in the jugular veins or in the descending aorta. The dynamic datasets were analyzed pixel-by-pixel using a modified Tofts model that took into account interstitial fluid pressure (4) or principal component analysis (5).

Results:

Control studies with the common extracellular contrast agent GdDTPA and with our control agent PTA-Gd showed enhancement in the rim and around the tumors, and barely in the central areas. The enhancement patterns in the rim were in accord with a two compartment physiological model, yielding the influx and outflux transcapillary transfer rate constants, with the later exceeding the former indicating the presence of high interstitial fluid pressure (6). In contrast, DCE-MRI of the ER targeted probes, EPTA-Gd and TPTA-Gd showed perfusion in the center of tumors and less outward convection. Both, the rim and core of the tumors were enhanced, despite the high IFP of these tumors. The difference in the perfusion distribution between the extracellular contrast agents and the ER targeted-intracellular agents suggests convection of the latter into the intracellular compartment rather than towards the outward environment. A significantly higher accumulation of EPTA-Gd was detected in the ER-positive tumors as compared to the ER-negative ones (Fig.2 a-c, Table 1) indicated binding to ER. The distribution of this agent over the entire tumor was heterogeneous suggesting heterogeneity of ER spatial expression; although we can not exclude the possibility that the high IFP could partially affect the delivery of the contrast agents. In contrast, TPTA-Gd accumulation in the ER-positive tumors was not significantly different from that in ER-

negative (Fig.2d). Unexpectedly, muscle tissue showed higher accumulation of TPTA-Gd than the tumors (Fig.2d) suggesting specific interaction of TPTA with muscle components independent of their ability to bind to ER.

In conclusion, the two ER-targeted probes had distinct kinetics in blood and in the tumors: EPTA-Gd pharmacokinetics in the blood was similar to that of the commonly used GdDTPA contrast agent, and was found to be effective in inducing specific contrast enhancement in ER-positive tumors and hence serve to detect ER. TPTA-Gd exhibited a long retention in the blood, and showed considerable accumulation in muscle tissue and was therefore not suitable for detecting ER *in vivo*.

References 1. Gunanathan C, Pais A et al. *Bioconjug Chem* 2007; 18(5):1361-1365. 2. Pais A et al. *ISMRM* 16th. Toronto, Canada, 2008. 3. Pais A et al. *ISMRM* 18th. Stockholm, Sweden, 2010. 4. Dadiani M et al. *Cancer Res* 2004; 64(9):3155-3161. 5. Eyal E et al. *J Magn Reson Imaging* 2009; 30(5):989-998. 6. Dadiani M et al. *Cancer Res* 2006; 66(16):8037-8041.

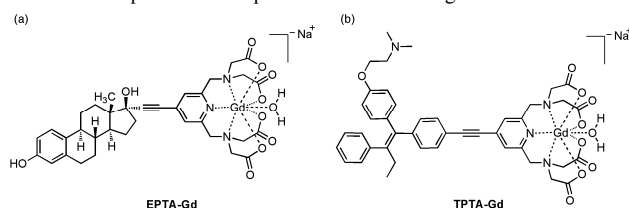


Figure 1. Schematic presentation of EPTA-Gd (a) and TPTA-Gd (b).

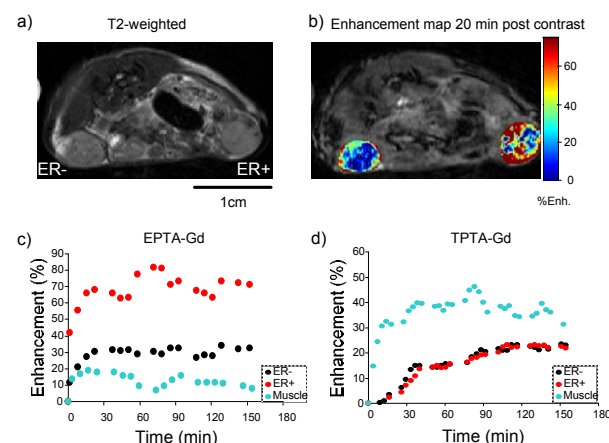


Figure 2. DCE-MRI of ER-negative and ER-positive MDA tumors with EPTA-Gd (a-c) and TPTA-Gd (d).

Table 1. Enhancement (%) over whole volume of ER- and ER+ MDA tumors at two time points after administration of ER-targeted probes to the tail vein of SCID mice. Data presented are mean \pm SEM.

Time post contrast	20-25 min			40-45 min		
	ER-	ER+	muscle	ER-	ER+	muscle
EPTA-Gd n=9	21.2 \pm 2.8	32.41 \pm 6.7		20.3 \pm 3.3	31.7 \pm 5.2	
	P=0.05			P=0.005		
TPTA-Gd n=4	13 \pm 8.8	10.9 \pm 2.2	27.2 \pm 3.9	19.4 \pm 5.2	12.2 \pm 0.6	28.4 \pm 3.2
	P=0.78			P=0.21		